The chromokinesin Kid forms a homodimer and moves processively along microtubules

Shinsuke Niwa[1,2,3,#], Natsuki Furusaki[2, 3], Tomoki Kita[2] and Kyoko Chiba[1,#]

1 Frontier Research Institute for Interdisciplinary Sciences (FRIS), Tohoku University, Miyagi 980-0845, Japan.

2 Graduate School of Life Sciences, Tohoku University, Miyagi 980-8577, Japan.

3 These authors equally contributed to this work

SHINSUKE NIWA, Frontier Research Institute for Interdisciplinary Sciences (FRIS), Tohoku University, Aramaki-Aoba 6-3, Aoba-Ku, Sendai, Miyagi 980-0845, Japan.

e-mail: shinsuke.niwa.c8@tohoku.ac.jp

KYOKO CHIBA, Frontier Research Institute for Interdisciplinary Sciences (FRIS), Tohoku University, Aramaki-Aoba 6-3, Aoba-Ku, Sendai, Miyagi 980-0845, Japan.

e-mail: kyoko.chiba.e7@tohoku.ac.jp

Abstract

During prometaphase in mitosis, chromosomes are pushed toward the spindle equator. The chromokinesin Kid moves chromosomes along spindle microtubules during prometaphase. Kid has long been considered as a monomeric and non-processive motor, different from typical kinesins that use two motor domains to transport cargos. However, this notion raises a question about how Kid transports chromosomes along microtubules. In this study, we demonstrate that the full-length Kid forms a homodimer and moves processively along microtubules. Both human and Xenopus Kid move along microtubules approximately at 70 nm/sec. We found Kid movement is characterized by frequent diffusive motions during the processive movement. Both human and Xenopus Kid, in their full-length forms, are eluted in dimer fractions in the size exclusion chromatography analysis but mostly dissociated into monomers in mass photometry analysis. A conserved coiled-coil domain within the stalk region of Kid is not only capable of homodimer formation, but is also required for the processivity of Kid. Furthermore, the stalk domain of Kid could add processive activity to the motor domain of KIF1A, suggesting that the stalk domain of Kid contains a functional neck linker and dimerization capability, a prerequisite for the processivity of kinesin motor domains. These findings collectively suggest the reclassification of Kid as a processive motor that possesses unique features.

Introduction

Microtubules are reorganized to form a bipolar spindle as cells enter mitosis. In the prometaphase of mitosis, chromosomes are transported along the microtubules toward the spindle equator (1) . This process, known as chromosome congression, requires kinesin-4, kinesin-10 and kinesin-12 class of motor proteins (2-4). The mechanical forces that move chromosomes toward the spindle equator is called polar ejection forces (1, 5, 6). The Kinesin-like DNA-binding protein (Kid), belonging to the kinesin-10 family and also known as KIF22, serves as a main molecular motor that transports chromosomes and generates polar ejection forces (5-10). Structurally, Kid contains a kinesin motor domain (11), a coiled-coil domain (12), and a DNA binding domain (8) (Figure 1A). In mitosis, the DNA binding domain of Kid binds along chromosome arms (6, 13, 14). Using the motor domain, Kid transports chromosomes (4, 5).

A single kinesin molecule can move for hundreds of steps along a microtubule without dissociating (15, 16). This property, called processivity, requires dimerization of kinesins (16). However, Kid has long been regarded as a monomeric and non-processive motor, which can move along microtubules in only a single step (11, 12). Consistent with these findings, Kid is unique within kinesin superfamily due to lack of the conventional neck coiled-coil domain (12) , an element that determines the length of the neck linker essential for the coordinated movement of the two motor domains (17-19). While a study has indicated the possibility that the full-length human Kid protein can move processively along microtubules (20), this study did not investigate the oligomeric state of Kid, nor did it provide detailed information on the Kid's motility characteristics and parameters. A Drosophila kinesin-10 motor NOD, an orthologue of Kid, is also characterized as a monomeric and non-processive motor (21). Similar to Kid, NOD has a DNA binding domain at the tail domain (22). NOD shows a processive movement only when the protein is forcedly dimerized by

the addition of an artificial coiled-coil domain (23). Nevertheless, Kid acts as an active motor in microtubule gliding assays and cargo transport assays, both of which detect movement generated by multiple Kid motors (4, 12, 24, 25). Collectively, it has been widely assumed that Kid, unlike other kinesins, transports chromosomes by their cooperative action of many non-processive monomers (3, 5, 10, 25).

Recently, we and others have analyzed properties of full-length kinesins (26-29). Notably, these studied have found that monomeric kinesins, including KIF1A, UNC-104 and KIF13B are converted to a dimer when activated (28, 30-32). For instance, in the autoinhibited and inactive state, KIF1A and UNC-104 are monomeric (30, 32). The monomeric motor domain of UNC-104 and KIF1A has a plus-end directed motor activity but exhibits one-dimensional diffusion, meaning that the efficiency is low (30, 33) . Upon the release of autoinhibition, KIF1A and UNC-104 form dimers, which exhibit efficient directional movement on microtubules (32). These studies prompted us to reanalyze the oligomeric state and the motile properties of Kid, mainly in the full length. In this study, we show that the full-length Kid protein moves processively along microtubules. Kid proteins can form dimers but Kid proteins are dissociated to monomers at low concentrations. Interestingly, Kid exhibits diffusive motions during its movement along microtubules, a characteristic that distinguishes it from other processive kinesins.

Results

Kid exhibits processive movement along microtubules

To study biochemical and biophysical properties of full-length Kid, we firstly purified the full-length human Kid (hKid) and Xenopus Kid (XKid) using the baculovirus system and Sf9 cells because a previous study has succeeded in purifying functional XKid from Sf9 cells (4) (14) (25). hKid as well as XKid possesses an N-terminal motor domain, a short coiled-coil domain and a DNA

binding tail domain (Figure 1A). Previous studies have shown that hKid and XKid, that are fused with fluorescent proteins at the C-terminal, can complement the function of hKid-depleted cells and XKid-depleted Xenopus egg extracts (4) (34). Thus, we fused a fluorescent protein at the C-terminal of XKid and hKid. Notably, while EGFP-fused and sfGFP-fused hKid were insoluble, mNeonGreen-fused hKid was recovered from soluble fractions. As a result, we succeeded in purifying both XKid-mScarlet and hKid-mNeonGreen proteins (Figure 1B, and supplemental Figure S1). Next, the motility of purified proteins were analyzed by single molecule motility assays using total internal reflection fluorescent microscopy (TIRF). We found that both XKid and hKid moved on microtubules processively (Figure 1C, D, Movie 1 and 2). The motility of single molecules along microtubules could be observed at 20 pM of Xkid and hKid, respectively. Interestingly, both XKid and hKid exhibited unstable fluctuations during the movement (movie 1 and 2), which is different from typical kinesins showing linear motion along the microtubules (26, 27, 35). The average velocity of XKid and hKid were approximately 70 nm/sec (Figure 1E and Table 1), within the same range as the movement of chromosomes (5). The run length of XKid and hKid were 4.11 ± 2.27 and 3.67 ± 2.16 µm, respectively (Figure 1F). These data collectively suggest that full-length Kid is a processive motor protein.

Full-length Kid form dimers

It has been proposed that Kid is a monomeric protein (11, 12). Even full-length human Kid protein obtained from 293T cells are indicated to be a monomer (12). However, typical kinesins show processive movement along microtubules only when they form dimers (16, 30, 32). As both hKid and XKid showed processive movement on microtubules (Fig 1), we next analyzed the oligomeric state of these motors using size exclusion chromatography (Figure 2). We utilized the previously well-characterized kinesin UNC-104(1-653)-sfGFP as a size marker.

UNC-104(1-653)-sfGFP exhibits a dimer peak at 200 kDa and a monomer peak at 100 kDa in size exclusion chromatography (32). This characteristic makes it a suitable marker for determining the oligomeric state of hKid and XKid, given that the predicted molecular weights of hKid-mNeonGreen and XKid-mScarlet monomers are approximately 100 kDa (Figure 1A). As a result, we found that the peak fraction of full-length hKid and XKid are almost equivalent to that of UNC-104(1-653)-sfGFP dimer (Fig 2A and B, and supplemental Figure S2). Notably, unlike UNC-104(1-653)-sfGFP, we did not detect any monomer peaks for hKid and XKid under these conditions. We next analyzed purified proteins recovered from the peak fractions using mass photometry (36). Mass photometry is generally performed at the nanomolar concentrations (36). Peak fractions obtained from size exclusion chromatography were diluted and analyzed. Mass photometry indicated the presence of significant amount of monomers (Figure 2C and D). The property is similar to the behavior of UNC-104(1-653)-sfGFP, which shows dimer peaks in the size exclusion chromatography at micromolar concentrations but dissociates into monomers at the nanomolar concentrations used for mass photometry (32). These findings indicate that full-length hKid and XKid are capable of forming dimers, but the dimer formation is dependent on the protein concentration.

A conserved coiled-coil domain is essential for the processivity

To determine the domain essential for the processive movement of Kid, we generated a series of deletion mutants. Unfortunately, we failed to purify adequate quantities and qualities of hKid deletion mutants. Thus, following experiments were performed using XKid. We purified XKid(1-495), which lacks the DNA-binding tail domain, and XKid(1-437), which lacks the DNA-binding domain and the coiled-coil domain (Figure 3A and B, and supplemental Figure S1). Using these purified proteins, we performed single molecule motility assays (Figure 3C-F). We

found XKid(1-495) could move processively on microtubules (Figure 3C). The velocity of XKid(1-495) was 70 nm/sec and the run length was 4.18 ± 1.56 µm, which are comparable to those of full-length XKid (Figure 3C-F, Table 1). Thus, DNA binding domain of Kid is not required for processive runs. In contrast, XKid(1-437), which lacks the coiled-coil domain, did not show any processive runs (Figure 3D). This would be because XKid(1-437) did not form a homodimer, considering that coiled-coil domains are generally required for the dimerization of kinesins (16, 32). To confirm that the coiled-coil domain of XKid induces dimerization, the domain was fused with mScarlet and analyzed by the size exclusion chromatography (Figure 3G). As a result, the peak of XKidCC-mScarlet shifted to the larger size compared with that of mScarlet. The calculated molecular weight of XKidCC-mScarlet was 42 kDa, which is almost equivalent to the size of dimerized mScarlet. These data suggest that the coiled-coiled domain of Kid can induce dimer formation.

The stalk domain of XKid adds processivity to the motor domain of KIF1A

In the processive movement along the microtubules, the coordination between two motor domains is essential (16). The neck linker domain, immediately following the kinesin motor domain, regulates the ATPase activity within the motor domain (18). It has been shown that optimal length of the neck linker domain is crucial for achieving coordination of the two motor domains (17, 19). The length of the neck linker domain is typically determined by the presence of the neck coiled-coil domain (18, 37) . Notably, Kid is an exception, as it does not have the conventional neck coiled-coil domain (8, 12). This unique feature of Kid supports the idea that Kid functions as a non-processive monomer (11), which does not require the coordination between two motor domains. However, coiled-coil prediction tools might not identify hidden coiled-coil domains or Kid could have a motif that induces dimerization. Notably, in the case of kinesin-1, Alphafold2, but not coiled-coil

prediction tools, can more accurately find the location of coiled-coil domains (38, 39). Therefore, we used Alphafold2 to analyze the neck-linker and the first coiled-coil domain of hKid and XKid. The result suggested that the region does not have hidden coiled-coil domains nor a motif that induces dimerization, and the region is flexible (Supplementary Figure S3). If the entire flexible region functions as a neck linker, its length is 4 times longer than that of kinesin-1 (Supplementary Figure S3) . To investigate if this unique stalk domain of Kid, which lacks the conventional neck coiled-coil domain yet possesses an extended neck linker, can support the coordination of two motor domains, we fused the stalk domain of XKid to the motor domain of KIF1A (Figure 4A). We included the possible neck linker domain of XKid in this chimera protein to test whether the neck linker of XKid is functional or not (Figure 4B). We could purify the chimeric protein, named KIF1AMD-XKidSt (Figure 4C and supplementary Figure S1). We found that KIF1AMD-XKidSt exhibited processive movement along microtubules in the single molecule motility assay (Figure 4D and movie S3). However, the motor showed occasional diffusions while they were moving along microtubules (Figure 4D and movie S3). This motile property was totally different from that of KIF1A(1-393)LZ showing typical linear movement (Figure 4E and movie S4). The velocity of KIF1AMD-XKidSt was much faster than original XKid but slightly slower than KIF1A(1-393)LZ (Figure 4F and Table 1). The run length of KIF1AMD-XKidSt was shorter than KIF1A(1-393)LZ (Figure 4G and Table 1). Previous studies have shown that the motor domain of KIF1A does not exhibit processive motion when it is monomeric, but exhibits processive motion when an artificial dimer is generated using a stalk domain of kinesin-1 or a leucine zipper domain (30, 35). Therefore, these results suggest that the stalk domain of XKid can induce dimerization of KIF1A motor domains on microtubules but the coordination between two motor domains are less organized compared to those of typical kinesins such as KIF1A.

Discussion

Kid is a processive motor protein on microtubules

Prometaphase chromosomes are transported along microtubules by the activity of kinesins (2, 3). Kid is the primary kinesin that transports chromosomes along spindle microtubules in prometaphase (3, 5). Our data show that full-length Kid is capable to form a dimer and exhibits a processive motion along microtubules, suggesting that Kid uses two motor domains and transports chromosomes along spindle microtubules as is the case in other kinesins (Figure 5A). A notable difference between this study and prior studies is the protein concentration used. Previous analysis of full-length human Kid via density gradient and size exclusion chromatography identified peak fractions through western blot, due to the low concentration of recombinant Kid expressed in 293T cells (12). We show that most hKid and XKid exist as dimers in size exclusion chromatography performed at micromolar concentrations, yet dissociate into monomers in mass photometry, which is performed at nanomolar concentrations (Figure 2). Thus, the inability to detect Kid dimers in earlier studies may be attributed to the low concentration. Another difference is the methods to detect the processivity of motors. We observed the processivity of Kid by TIRF whereas previous studies observed the motility by optical trap. In optical trapping assays, Kid is diluted prior to being adsorbed onto beads. This dilution process results in the dissociation of dimerized Kid, thereby predominantly observing the motility of monomeric Kid in the assay. Conversely, in TIRF-based motility assays, although Kid predominantly dissociates into monomers in solution, its direct interaction with microtubules leads to an increased local concentration of Kid on the microtubule surface. As a result, this would facilitate the formation of Kid dimers on the microtubules, leading to processive motility. These properties, such as 'the equilibrium between monomers and dimers' and 'the capability to exhibit processive movement on microtubules, even when characterized as monomers through mass photometry,' have been observed in kinesin-3 motors (28, 31, 32).

Kid may be optimized for chromosome transport

Unlike vesicular cargos, which can change their shapes in the cytoplasm while they are transported (40), prometaphase chromosomes require the preservation of their shapes and structural integrity throughout the transport process. Therefore, it has been proposed that motor proteins that transport chromosomes should have a slow and weak properties to ensure precise delivery, because fast processive motors could potentially disrupt chromosomes during metaphase (5). Indeed, another chromosomal motor CENP-E is a very slow motor (41). This concept aligns with the observed properties of full-length Kid motors in this study. We show that Kid is characterized by a slow speed and presence of diffusive fluctuations during movement (Figure 5B). A prior study has shown that prometaphase chromosomes are transported by a motor protein which moves at 63 ± 41 nm/sec (5). The value is very well fit with the velocity of full-length Kid dimers observed in this study.

The characteristics of Kid are thought to be determined by the unique structure of Kid. Because the chimeric protein composed of the motor domain of KIF1A and the stalk domain of XKid is much faster than original Kid proteins, the very slow motility of Kid is mainly attributed to the property of the motor domain of Kid. On the other hand, the tendency to exhibit diffusions is linked to the stalk domain of Kid, as the chimeric protein displays similar diffusions that is not observed in original KIF1A. In typical kinesins, the length of neck linker is optimized for the coordinated action between the two motor domains. Although the length of the neck linker is determined by the neck coiled-coil domain, Kid does not have a conventional neck coiled-coil domain (12) (Figure 4B, supplementary Figure S3). Indeed, it has been shown that an artificial kinesin-1 (KIF5) with a longer neck linker exhibits diffusive motions during the movement along microtubules (17, 19). Therefore, occasional diffusions during the movement of Kid is attributed to the absence of the conventional neck coiled-coil domain, which disorganizes the coordination

between two motor domains. These features of Kid proteins appears to be a drawback as a transporter but would be acquired for the gentle transport of prometaphase chromosomes.

Methods

Plasmids

PCR was performed using a KOD FX neo DNA polymerase (TOYOBO, Tokyo, Japan). Human Kid cDNA (corresponding to DQ895829.2) was described previously (3). Xenopus Kid (Kif22.S, corresponding to BC070549.1) was purchased from Horizon Discovery. To generate hKidFL-mNeonGreen, DNA fragments encoding human Kid and mNeonGreen were amplified by PCR and assembled into pFastbac1 (Novagen) by Gibson assembly as described (42). To generate XKidFL-mScarlet, DNA fragments encoding XKid and mScarlet were amplified by PCR and assembled into pAcebac1 (Geneva Biotech). ORF sequences are shown in Supplementary Table S1. Deletion mutants of XKid were generated by PCR-based mutagenesis. For this purpose, primers were designed through the QuickChange Primer Design tool, a web-based application (Agilent). PCR-based mutagenesis was performed using KOD plus neo DNA polymerase (TOYOBO).

Expression of XKid and Kid in Sf9 cells

Sf9 cells (Thermo Fisher Scientific) were maintained in Sf900™ II SFM (Thermo Fisher Scientific) at 27°C. DH10Bac (Thermo Fisher Scientific) were transformed to generate bacmid. To prepare baculovirus, 1×10^6 cells of Sf9 cells were transferred to each well of a tissue-culture treated 6 well plate. After the cells attached to the bottom of the dishes, about ~5 μg of bacmid were transfected using 5 μL of TransIT®-Insect transfection reagent (Takara Bio Inc.). 5 days after initial transfection, the culture media were collected and spun at 3,000 × g for 3 min to obtain the supernatant (P1). For protein expression, 400 mL of Sf9 cells (2×10^6 cells/mL) were infected with

200 µL of P1 virus and cultured for 65 h at 27°C. Cells were harvested and stocked at -80°C.

Purification of proteins

We failed to purify hKid-EGFP and hKid-superfolder GFP due to the insolubility. In contrast, mNeonGreen fusion stabilized hKid and enabled purification.

Sf9 cells were resuspended in 40 mL of Kid lysis buffer (50 mM HEPES-KOH, pH 7.5, 500 mM KCH3COO, 2 mM MgSO4, 1 mM EGTA, 10% glycerol) along with 1 mM DTT, 1 mM PMSF, 0.1 mM ATP and 0.5% Triton X-100. After incubating on ice for 10 min, lysates were cleared by centrifugation (100,000 × g, 20 min, 4°C) and subjected to affinity chromatography. Lysate was loaded on Streptactin-XT resin (IBA Lifesciences, Göttingen, Germany) (bead volume: 2 ml). The resin was washed with 40 ml Kid wash buffer (50 mM HEPES-KOH, pH 8.0, 500 mM KCH_3COO, 2 mM $MgSO_4$, 1 mM EGTA, 10% glycerol). Protein was eluted with 40 ml Kid elution buffer (50 mM HEPES-KOH, pH 8.0, 500 mM KCH_3COO, 2 mM $MgSO_4$, 1 mM EGTA, 10% glycerol, 200 mM biotin). Eluted solution was concentrated using an Amicon Ultra 15 (Merck) and then separated on an NGC chromatography system (Bio-Rad) equipped with a Superdex 200 Increase 10/300 GL column (Cytiva). Peak fractions were collected and concentrated using an Amicon Ultra 4 (Merck). Proteins were analyzed by SDS-PAGE using TGX Stain-Free gel (Bio-Rad). Concentrated proteins were aliquoted and snap-frozen in liquid nitrogen.

Mass photometry

Purified hKid and XKid obtained from the peak fractions in the SEC analysis were pooled, snap-frozen and stored until measurement. Prior to measurement, the proteins were thawed and diluted to a final concentration 5 nM in GF150 buffer (25 mM HEPES, 150 mM KCl, 2 mM $MgCl_2$, pH 7.2). Mass photometry was performed using a Refeyn OneMP mass photometer (Refeyn) and

Refeyn AcquireMP version 2.3 software, with default parameters set by Refeyn AcquireMP. Bovine serum albumin (BSA) was used as a control to determine the molecular weight. The results were subsequently analyzed and graphs were prepared to visualize the data using Refeyn DiscoverMP version 2.3.

Preparation of microtubules

Tubulin was purified from porcine brain as described (43). Tubulin was labeled with Biotin-PEG$_2$-NHS ester (Tokyo Chemical Industry, Tokyo, Japan) and AZDye647 NHS ester (Fluoroprobes, Scottsdale, AZ, USA) as described (44). To polymerize Taxol-stabilized microtubules labeled with biotin and AZDye647, 30 μM unlabeled tubulin, 1.5 μM biotin-labeled tubulin and 1.5 μM AZDye647-labeled tubulin were mixed in BRB80 buffer supplemented with 1 mM GTP and incubated for 15 min at 37°C. Then, an equal amount of BRB80 supplemented with 40 μM taxol was added and further incubated for more than 15 min. The solution was loaded on BRB80 supplemented with 300 mM sucrose and 20 μM taxol and ultracentrifuged at 100,000 g for 5 min at 30°C. The pellet was resuspended in BRB80 supplemented with 20 μM taxol.

TIRF single-molecule motility assays

Purified Kid proteins described above were thawed and analyzed. KIF1A (1-393)LZ, that was described in our previous work (45), was also thawed and reanalyzed. TIRF assays using porcine microtubules were performed as described (27). Glass chambers were prepared by acid washing as previously described (26). Glass chambers were coated with PLL-PEG-biotin (50% labelled, SuSoS, Dübendorf, Switzerland) and streptavidin (Wako). Polymerized microtubules were flowed into flow chambers and allowed to adhere for 5–10 min. Unbound microtubules were washed away using assay buffer (90 mM HEPES-KOH pH 7.4, 50 mM KCH_3COO, 2 mM $Mg(CH_3COO)_2$,

1 mM EGTA, 10% glycerol, 0.1 mg/ml biotin–BSA, 0.2 mg/ml kappa-casein, 0.5% Pluronic F127, 2 mM ATP, and an oxygen scavenging system composed of PCA/PCD/Trolox). Purified Kid was diluted to indicated concentrations in the assay buffer. Then, the solution was flowed into the glass chamber. An ECLIPSE Ti2-E microscope equipped with a CFI Apochromat TIRF 100XC Oil objective lens (1.49 NA), an Andor iXion life 897 camera and a Ti2-LAPP illumination system (Nikon, Tokyo, Japan) was used to observe the motility. NIS-Elements AR software ver. 5.2 (Nikon) was used to control the system. At least three independent experiments were conducted for each measurement.

Alphafold2 analysis

Alphafold2 analysis was conducted on Google Colaboratory (46, 47) . We analyzed the amino acid sequences of KIF5C, XKid, and hKid, ranging from the neck linker to the end of coiled-coil 1. The sequences are detailed in Supplementary Table S2. The analysis was based on the assumption that these fragments form dimers and XKid and hKid fold in the similar manner.

Statistical analyses and graph preparation

Statistical analyses and graph preparation were conducted using GraphPad Prism version 10. Details on the statistical methods are provided in the figure legends. Graphs were created with GraphPad Prism version 10, exported in PDF format, and aligned using Adobe Illustrator 2023.

Acknowledgments

We would like to thank the members of Niwa lab for useful discussions. We also would like to thank Dr. Atsushi Nakagawa and Mr. Jiye Wang (Osaka University) for technical assistance.

SN was supported by JSPS KAKENHI (grant no. JP23H02472). TK was supported by JSPS KAKENHI (grant no. JP23KJ0168). KC was supported by JSPS KAKENHI (grant no. JP22K15053), Uehara Memorial Foundation, Naito Foundation and MEXT Leading Initiative for Excellent Researchers (grant no. JPMXS0320200156). This work was performed under the Collaborative Research Program of Institute for Protein Research, Osaka University, CR-23-02.

Author contributions

Shinsuke Niwa: Conceptualization; Resources; Data curation; Formal analysis; Project administration; Supervision; Funding acquisition; Validation; Investigation; Visualization; Methodology; Writing—original draft; Writing—review and editing.

Natsuki Furusaki: Resources; Data curation; Formal analysis; Validation; Investigation

Tomoki Kita: Resources; Data curation; Formal analysis; Validation; Investigation

Kyoko Chiba: Resources; Data curation; Formal analysis; Supervision; Funding acquisition; Project administration; Writing—review and editing.

Conflict of interest

The authors declare no competing interests.

Statement

During the preparation of this work the authors used GPT4.0 in order to check English grammar and improve English writing. After using this tool, the authors reviewed and edited the content as needed and take full responsibility for the content of the publication.

References

1. C. L. Rieder, E. A. Davison, L. C. Jensen, L. Cassimeris, E. D. Salmon, Oscillatory movements of monooriented chromosomes and their position relative to the spindle pole result from the ejection properties of the aster and half-spindle. *J Cell Biol* **103**, 581-591 (1986).
2. L. Wordeman, How kinesin motor proteins drive mitotic spindle function: Lessons from molecular assays. *Semin Cell Dev Biol* **21**, 260-268 (2010).
3. K. Iemura, K. Tanaka, Chromokinesin Kid and kinetochore kinesin CENP-E differentially support chromosome congression without end-on attachment to microtubules. *Nat Commun* **6**,

6447 (2015).

4. P. Bieling, I. Kronja, T. Surrey, Microtubule motility on reconstituted meiotic chromatin. *Curr Biol* **20**, 763-769 (2010).
5. G. J. Brouhard, A. J. Hunt, Microtubule movements on the arms of mitotic chromosomes: polar ejection forces quantified in vitro. *Proc Natl Acad Sci U S A* **102**, 13903-13908 (2005).
6. A. A. Levesque, D. A. Compton, The chromokinesin Kid is necessary for chromosome arm orientation and oscillation, but not congression, on mitotic spindles. *J Cell Biol* **154**, 1135-1146 (2001).
7. M. Ohsugi *et al.*, Cdc2-mediated phosphorylation of Kid controls its distribution to spindle and chromosomes. *EMBO J* **22**, 2091-2103 (2003).
8. N. Tokai *et al.*, Kid, a novel kinesin-like DNA binding protein, is localized to chromosomes and the mitotic spindle. *EMBO J* **15**, 457-467 (1996).
9. C. Wandke *et al.*, Human chromokinesins promote chromosome congression and spindle microtubule dynamics during mitosis. *J Cell Biol* **198**, 847-863 (2012).
10. A. F. Thompson *et al.*, Pathogenic mutations in the chromokinesin KIF22 disrupt anaphase chromosome segregation. *Elife* **11** (2022).
11. J. Yajima *et al.*, The human chromokinesin Kid is a plus end-directed microtubule-based motor. *EMBO J* **22**, 1067-1074 (2003).
12. K. Shiroguchi, M. Ohsugi, M. Edamatsu, T. Yamamoto, Y. Y. Toyoshima, The second microtubule-binding site of monomeric kid enhances the microtubule affinity. *J Biol Chem* **278**, 22460-22465 (2003).
13. C. Antonio *et al.*, Xkid, a chromokinesin required for chromosome alignment on the metaphase plate. *Cell* **102**, 425-435 (2000).
14. H. Funabiki, A. W. Murray, The Xenopus chromokinesin Xkid is essential for metaphase chromosome alignment and must be degraded to allow anaphase chromosome movement. *Cell* **102**, 411-424 (2000).
15. D. D. Hackney, Highly processive microtubule-stimulated ATP hydrolysis by dimeric kinesin head domains. *Nature* **377**, 448-450 (1995).
16. W. O. Hancock, J. Howard, Processivity of the motor protein kinesin requires two heads. *J Cell Biol* **140**, 1395-1405 (1998).
17. H. Isojima, T. Mori, M. Tomishige, Optimal Size of the Neck Linker is Important for the Coordinated Processive Movement of Kinesin-1. *Biophysical Journal* **98**, 369a-369a (2010).
18. R. B. Case, S. Rice, C. L. Hart, B. Ly, R. D. Vale, Role of the kinesin neck linker and catalytic core in microtubule-based motility. *Curr Biol* **10**, 157-160 (2000).
19. A. Yildiz, M. Tomishige, A. Gennerich, R. D. Vale, Intramolecular strain coordinates kinesin stepping behavior along microtubules. *Cell* **134**, 1030-1041 (2008).

20. J. Stumpff, M. Wagenbach, A. Franck, C. L. Asbury, L. Wordeman, Kif18A and chromokinesins confine centromere movements via microtubule growth suppression and spatial control of kinetochore tension. *Dev Cell* **22**, 1017-1029 (2012).
21. H. J. Matthies, R. J. Baskin, R. S. Hawley, Orphan kinesin NOD lacks motile properties but does possess a microtubule-stimulated ATPase activity. *Mol Biol Cell* **12**, 4000-4012 (2001).
22. K. Afshar, N. R. Barton, R. S. Hawley, L. S. Goldstein, DNA binding and meiotic chromosomal localization of the Drosophila nod kinesin-like protein. *Cell* **81**, 129-138 (1995).
23. A. A. Ye, V. Verma, T. J. Maresca, NOD is a plus end-directed motor that binds EB1 via a new microtubule tip localization sequence. *J Cell Biol* **217**, 3007-3017 (2018).
24. C. Li, C. Xue, Q. Yang, B. C. Low, Y. C. Liou, NuSAP governs chromosome oscillation by facilitating the Kid-generated polar ejection force. *Nat Commun* **7**, 10597 (2016).
25. J. Takagi, T. Itabashi, K. Suzuki, S. Ishiwata, Chromosome position at the spindle equator is regulated by chromokinesin and a bipolar microtubule array. *Sci Rep* **3**, 2808 (2013).
26. K. Chiba, K. M. Ori-McKenney, S. Niwa, R. J. McKenney, Synergistic autoinhibition and activation mechanisms control kinesin-1 motor activity. *Cell Rep* **39**, 110900 (2022).
27. K. Chiba *et al*., Disease-associated mutations hyperactivate KIF1A motility and anterograde axonal transport of synaptic vesicle precursors. *Proc Natl Acad Sci U S A* **116**, 18429-18434 (2019).
28. X. M. Fan, R. J., Control of motor landing and processivity by the CAP-Gly domain in the KIF13B tail. *Nat Commun* **14**, 4715 (2022).
29. W. Wang, J. Ren, W. Song, Y. Zhang, W. Feng, The architecture of kinesin-3 KLP-6 reveals a multilevel-lockdown mechanism for autoinhibition. *Nat Commun* **13**, 4281 (2022).
30. M. Tomishige, D. R. Klopfenstein, R. D. Vale, Conversion of Unc104/KIF1A kinesin into a processive motor after dimerization. *Science* **297**, 2263-2267 (2002).
31. K. Chiba, T. Kita, Y. Anazawa, S. Niwa, Insight into the regulation of axonal transport from the study of KIF1A-associated neurological disorder. *J Cell Sci* **136** (2023).
32. T. Kita, K. Chiba, J. Wang, A. Nakagawa, S. Niwa, Comparative analysis of two Caenorhabditis elegans kinesins KLP-6 and UNC-104 reveals a common and distinct activation mechanism in kinesin-3. *Elife* **12** (2024).
33. Y. Okada, H. Higuchi, N. Hirokawa, Processivity of the single-headed kinesin KIF1A through biased binding to tubulin. *Nature* **424**, 574-577 (2003).
34. S. Soeda, K. Yamada-Nomoto, M. Ohsugi, The microtubule-binding and coiled-coil domains of Kid are required to turn off the polar ejection force at anaphase. *J Cell Sci* **129**, 3609-3619 (2016).
35. V. Soppina *et al.*, Dimerization of mammalian kinesin-3 motors results in superprocessive motion. *Proc Natl Acad Sci U S A* **111**, 5562-5567 (2014).

36. A. Sonn-Segev *et al.*, Quantifying the heterogeneity of macromolecular machines by mass photometry. *Nat Commun* **11**, 1772 (2020).
37. S. Shastry, W. O. Hancock, Neck linker length determines the degree of processivity in kinesin-1 and kinesin-2 motors. *Curr Biol* **20**, 939-943 (2010).
38. Z. Tan *et al.*, Autoinhibited kinesin-1 adopts a hierarchical folding pattern. *elife* **12**, RP86776 (2023).
39. J. F. Weijman *et al.*, Molecular architecture of the autoinhibited kinesin-1 lambda particle. *Sci Adv* **8**, eabp9660 (2022).
40. T. Nakata, S. Terada, N. Hirokawa, Visualization of the dynamics of synaptic vesicle and plasma membrane proteins in living axons. *J Cell Biol* **140**, 659-674 (1998).
41. Y. Kim, J. E. Heuser, C. M. Waterman, D. W. Cleveland, CENP-E combines a slow, processive motor and a flexible coiled coil to produce an essential motile kinetochore tether. *J Cell Biol* **181**, 411-419 (2008).
42. D. G. Gibson *et al.*, Enzymatic assembly of DNA molecules up to several hundred kilobases. *Nat Methods* **6**, 343-345 (2009).
43. M. Castoldi, A. V. Popov, Purification of brain tubulin through two cycles of polymerization-depolymerization in a high-molarity buffer. *Protein Expr Purif* **32**, 83-88 (2003).
44. J. Al-Bassam, Reconstituting Dynamic Microtubule Polymerization Regulation by TOG Domain Proteins. *Methods in Enzymology* **540**, 131-148 (2014).
45. Y. Anazawa, T. Kita, R. Iguchi, K. Hayashi, S. Niwa, De novo mutations in KIF1A-associated neuronal disorder (KAND) dominant-negatively inhibit motor activity and axonal transport of synaptic vesicle precursors. *Proc Natl Acad Sci U S A* **119**, e2113795119 (2022).
46. J. Jumper *et al.*, Highly accurate protein structure prediction with AlphaFold. *Nature* **596**, 583-589 (2021).
47. M. Mirdita *et al.*, ColabFold: making protein folding accessible to all. *Nat Methods* **19**, 679-682 (2022).

Figure legends

Figure 1 Kid is a processive motor

(A) Schematic illustration of the domain organization in Xenopus Kid tagged with a fluorescent protein mScarlet (XKidFL) and human Kid tagged with mNeonGreen (hKidFL). The calculated molecular weights of the fusion proteins are indicated on the right.

(B) Representative SDS-PAGE analysis of purified XKidFL and hKidFL fusion proteins. The proteins are visualized using a Stain-Free gel. The molecular weight standards are indicated on the left side of the SDS-PAGE images.

(C and D) Representative kymographs showing the motility of XKidFL at 20 pM (C) and hKidFL at

20 pM (D) both in the presence of 2 mM ATP. Scale bars: horizontal, 10 µm; vertical, 60 seconds.

(E) Dot plots showing the velocity of XKidFL and hKidFL. Each dot shows a single datum point. Green bars represent mean ± S.D.. n = 71, respectively.

(F) Dot plots showing the run length of XKidFL and hKidFL. Each dot shows a single datum point. Green bars represent mean ± S.D.. n = 70, respectively.

Figure 2 Kid forms a weak dimer

(A) Size exclusion chromatography profiles of hKidFL (black) and UNC-104(1-653)-sfGFP (cyan). Below the chromatography, an SDS-PAGE image show the elution fractions. Asterisks indicate fractions used for mass photometry and single molecule assays. The molecular weight standards are indicated on the left side of the SDS-PAGE images.

(B) Size exclusion chromatography of XKidFL (black) and UNC-104(1-653) (cyan). The SDS-PAGE of the elution fractions are shown beneath the profiles. Asterisks indicate fractions used for mass photometry and single molecule assays. The number shown at the left side indicates molecular weight standard.

(C) Mass photometry of human Kid. Histograms show the number of counts at 5 nM. Lines show Gaussian fits (mean ± S.D.: 110 ± 21 kDa and 211 ± 21 kDa, respectively).

(D) Mass photometry of Xenopus Kid. Histograms show the number of counts at 5 nM. Lines show Gaussian fits (mean ± S.D.: 117 ± 33 kDa and 208 ± 49 kDa, respectively).

Note that majority of hKid and XKid are dimers in the size exclusion chromatography but they are mostly dissociated to monomers in mass photometry.

Figure 3 Conserved coiled-coil domain is required for the processive motion

(A) Schematic representation illustrating the domain organization of XKid(1-495) and XKid(1-437).

(B) Representative SDS-PAGE analysis of purified XKid(1-495) and XKid(1-437) proteins. The proteins are visualized using a Stain-Free gel. The molecular weight standards are indicated on the right side of the SDS-PAGE images.

(C and D) Representative kymographs showing the motility of 20 pM XKid(1-495) (C) and XKid(1-437) (D) in the presence of 2 mM ATP. Note that no directional movement was detected in XKid(1-437). Scale bars: horizontal 5 µm; vertical 60 seconds.

(E) Dot plots showing the velocity of XKid(1-495) and XKid(1-437). Each dot represents an individual measurement of velocity. Green bars represent mean ± S.D.. n= 57 particles for XKid(1-495). nd, not detected.

(F) Dot plots showing the run length of XKid(1-495) and XKid(1-437). Each dot shows a single datum point. Green bars represent mean ± S.D.. n = 57 particles for XKid(1-495). nd, not detected.

(G and H) Schematic drawing of XKidCC-mScarlet (G) and a representative result of size exclusion

chromatography (H). XKidCC-mScarlet (magenta) and mScarlet (cyan) are shown.

Figure 4 The diffusive motion of Kid is attributed to the stalk domain

(A) Schematic representation illustrating the domain organization of KIF1A(1-393)LZ, XKid(1-495), KIF1A(1-350) and a chimera protein KIF1AMD-XKidSt. Note that KIF1A(1-393)LZ and XKid(1-495) are processive motors and KIF1A(1-350) is a non-processive motor. Cyan, motor domain of KIF1A; Orange, motor domain of Kid; Magenta, neck linker.

(B) Amino acid sequences of the neck linker region. KIF1A, XKid, hKid, KIF5C and KIF1AMD-XKidSt are shown. Cyan, motor domain of KIF1A and KIF5C; Orange, motor domain of Kid; Magenta, neck linker; Green, neck coiled-coil domain.

(C) Representative SDS-PAGE analysis of purified KIF1AMD-XKidSt fusion protein. The protein is visualized using a Stain-Free gel. The molecular weight standards are indicated on the right side of the SDS-PAGE image.

(D and E) Representative kymographs showing the motility of KIF1AMD-XKidSt and KIF1A(1-393)LZ in the presence of 2 mM ATP. Note that KIF1AMD-XKidSt exhibits diffusion-like fluctuations while they are moving. This phenomena is not observed in KIF1A(1-393)LZ. Scale bars: horizontal 10 µm; vertical 10 seconds.

(F) Dot plots showing the velocity of KIF1AMD-XKidSt and KIF1A(1-393)LZ. Each dot shows a single datum point. Green bars represent mean ± S.D.. ****, $p < 0.0001$, Unpaired t-test. $n = 273$ and 434 particles for KIF1AMD-XKidSt and KIF1A(1-393)LZ, respectively.

(G) Dot plots showing the run length of KIF1AMD-XKidSt and KIF1A(1-393)LZ. Each dot shows a single datum point. Green bars represent median value and interquartile range. ****, $p < 0.0001$, Mann-Whitney test. $n = 273$ and 434 particles for KIF1AMD-XKidSt and KIF1A(1-393)LZ, respectively.

Figure 5 Model

(A) Kid forms dimers and transports chromosomes along prometaphase spindle microtubules.

(B) Each Kid dimer functions as a slow and processive motor, which is characterized by a tendency to exhibit diffusive motions. These properties are different from typical kinesins that transport vesicular organelles and protein complexes.

	Processive	Oligomeric state in SEC	Velocity (μm/sec)	Run length (μm)
Full length hKid	Yes	Dimer	0.0671 ± 0.0319	4.11 ± 2.27
Full length XKid	Yes	Dimer	0.0646 ± 0.0247	3.67 ± 2.16
XKid(1-495)	Yes	Dimer	0.0646 ± 0.0266	4.18 ± 1.56
XKid(1-437)	No	Monomer	nd	nd
KIF1A(1-393)LZ	Yes	Dimer	1.37 ± 0.44	11.1 ± 10.9
KIF1AMD-XKidSt	Yes	Dimer	0.67 ± 0.18	6.67 ± 6.02

Table 1 Motile properties of constructs used in this study

Motor protein constructs underwent purification through affinity chromatography followed by size exclusion chromatography, as detailed in the Materials and Methods section. The reported velocities and run lengths represent mean values ± standard deviation (SD). Notably, XKid(1-437) failed to demonstrate consistent processive motion across three separate protein preparations, indicating a lack of detectable activity (ND: not detected).

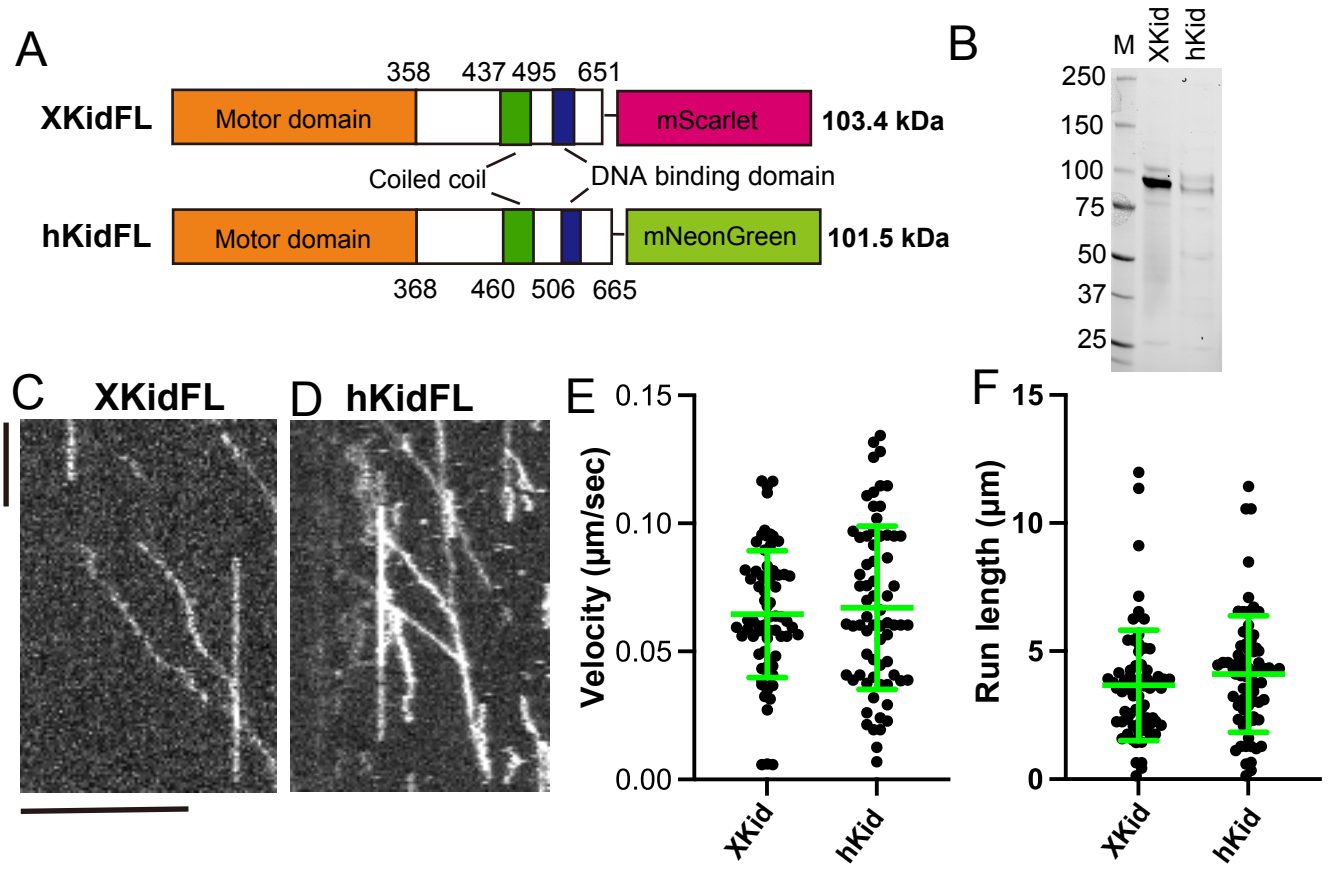

Niwa and Furusaki et al. Figure 1

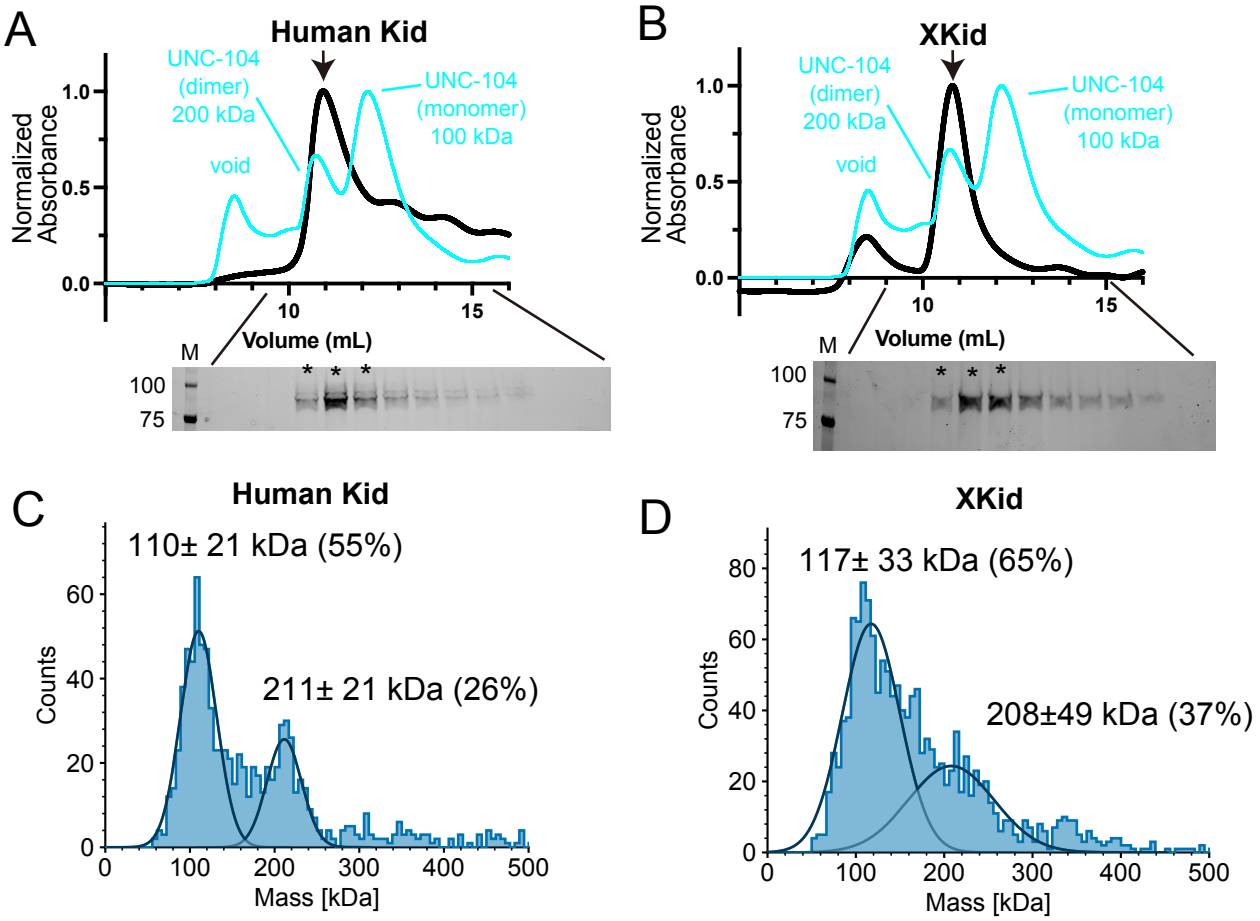

Niwa and Furusaki et al. Figure 2

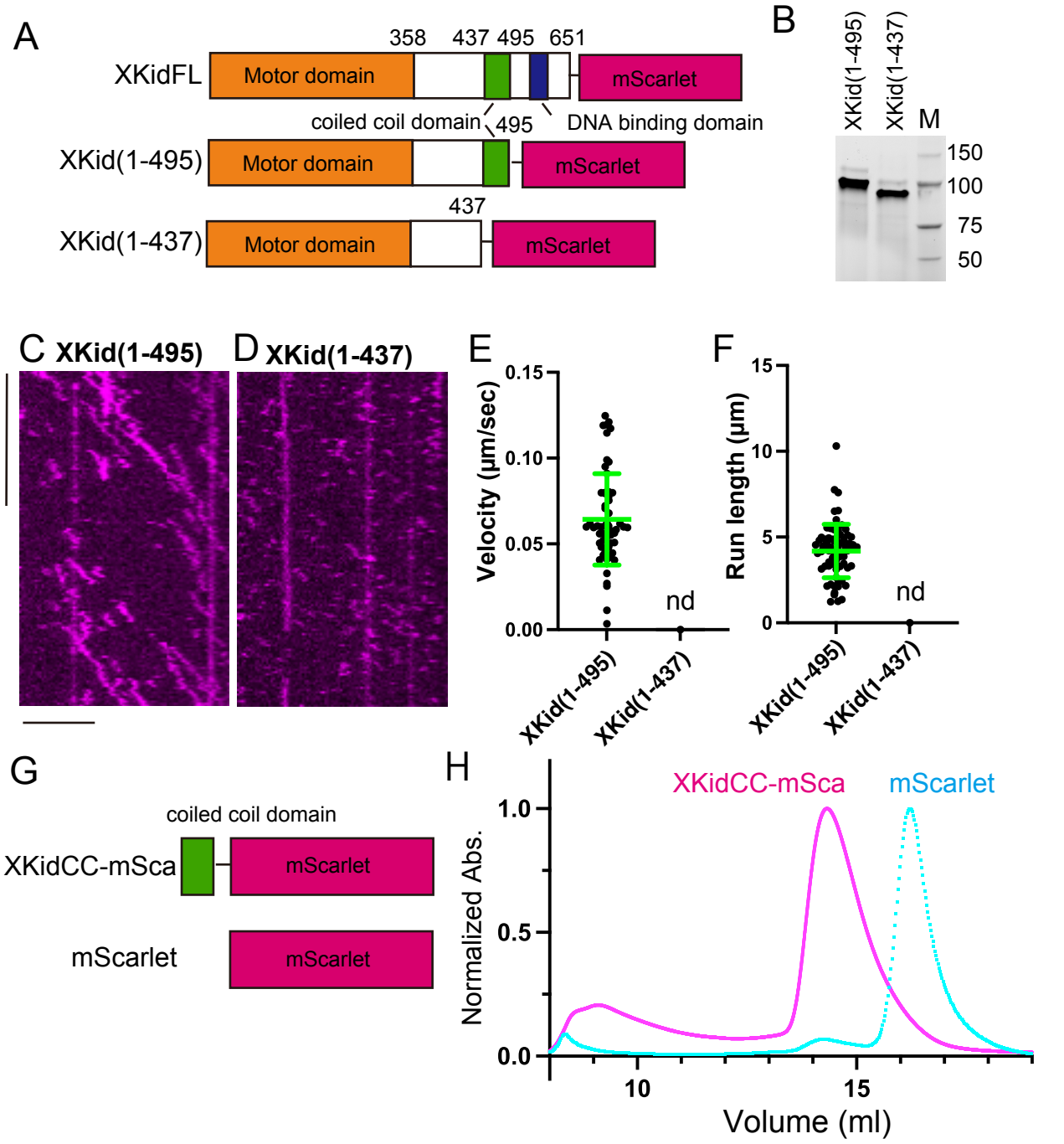

Niwa and Furusaki et al. Figure 3

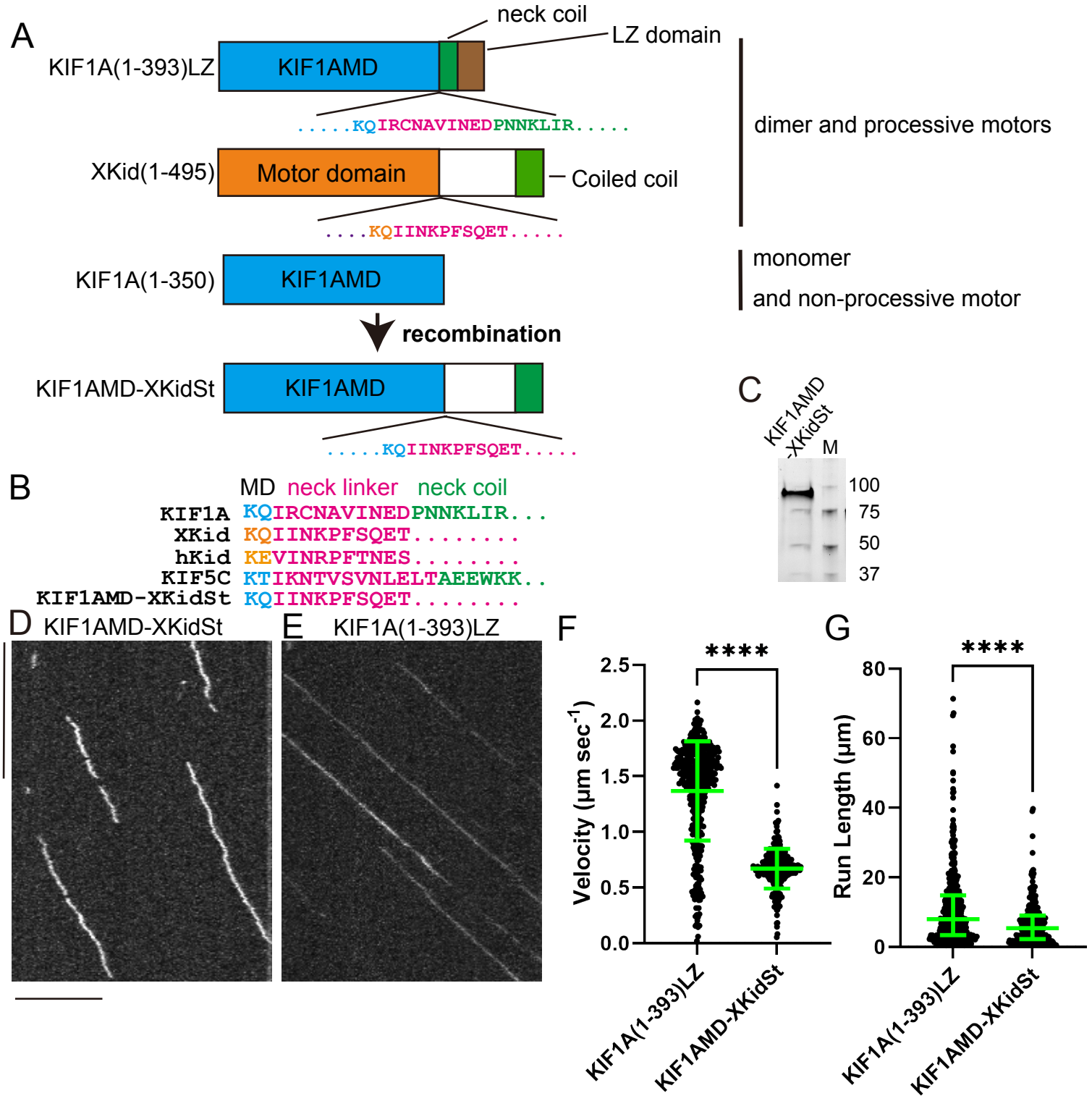

Niwa and Furusaki et al. Figure 4

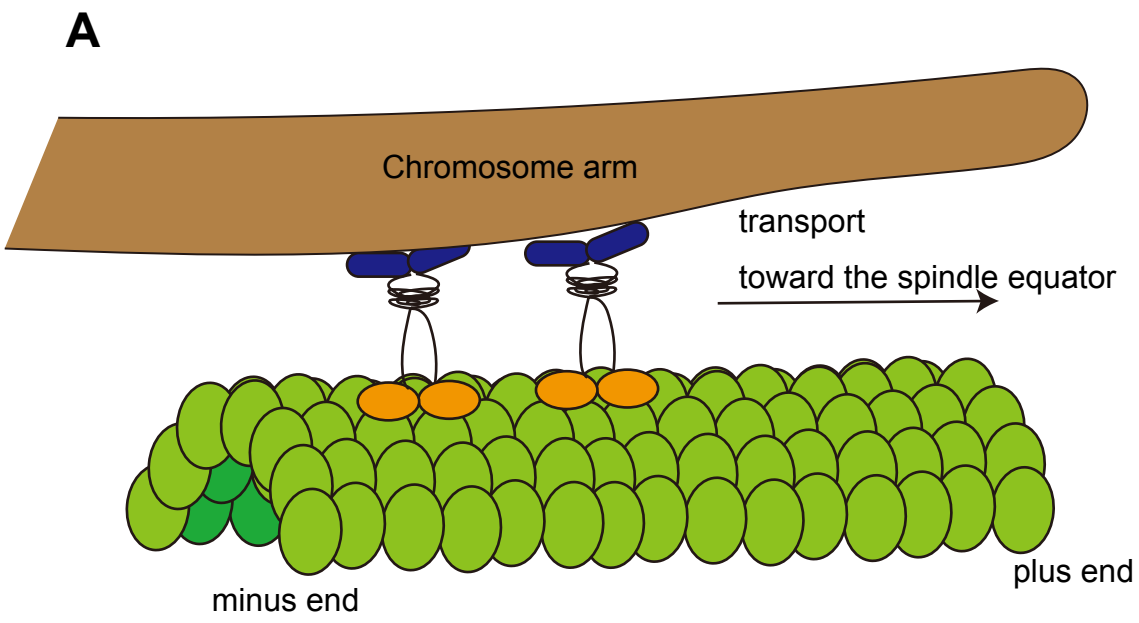

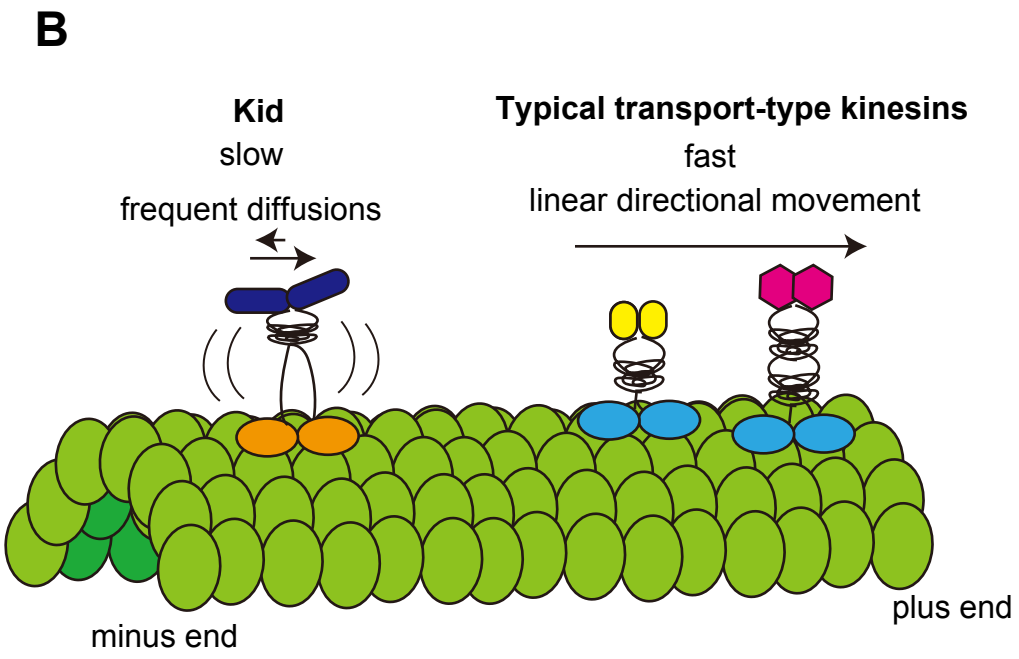

Niwa and Furusaki et al. Figure 5